Electronic Supplementary Information

Semiconductive donor promoted photochromism of iodoplumbate hybrids

Junju Shen, Xiaoli Kang, Pengfei Hao and Yunlong Fu*

Key Laboratory of Magnetic Molecules & Magnetic Information Materials Ministry of Education, School of Chemistry & Material Science, Shanxi Normal University, Linfen 041004, China.

*Corresponding author.

E-mail: yunlongfu@sxnu.edu.cn

Contents

1. Figures 2

Fig. S1 Thermogravimetric (TG) curves of **1** and **2** 2

Fig. S2 The asymmetric units of **1** and **2** 3

Fig. S3 Powder X-ray diffraction (PXRD) patterns of **1** and **2** 4

Fig. S4 UV-vis absorption spectra of **1** and **2** before and after irradiation 5

Fig. S5 Optical band gaps of **1** and **2** 6

Fig. S6 IR spectra of **1** and **2** before and after irradiation 7

Fig. S7 The calculated UV-vis spectra of $[MNH]^{2+}$ cation and $[MNH]^{+\bullet}$ radical 8

Fig. S8 EPR spectra of **2** before and after irradiation 8

2. Tables 9

Table S1 Crystallographic data and refinement parameters of **1** and **2** 9

Table S2 Selected distances (Å) and angles (°) of **1** and **2** 10

Table S3 Density functional theory (DFT) calculations for two cations 11

Reference 12

1. Figures

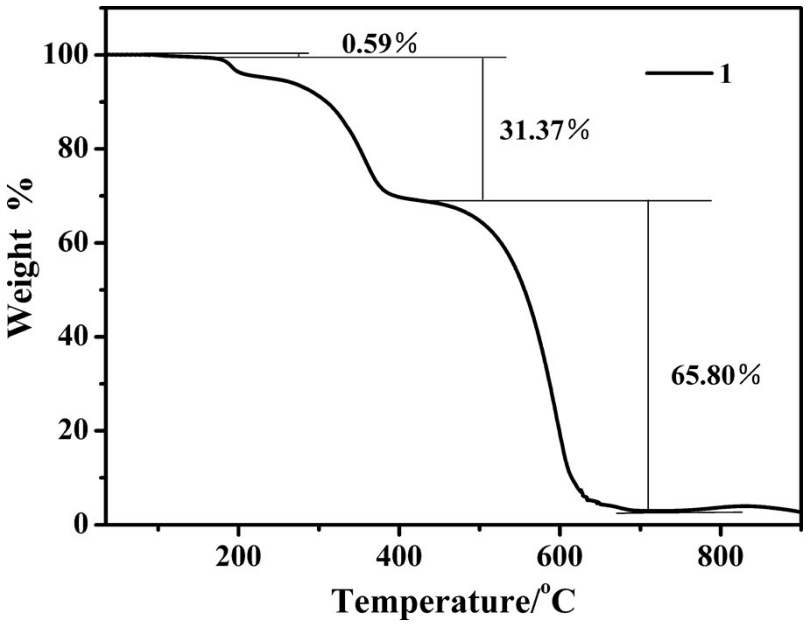

(a)

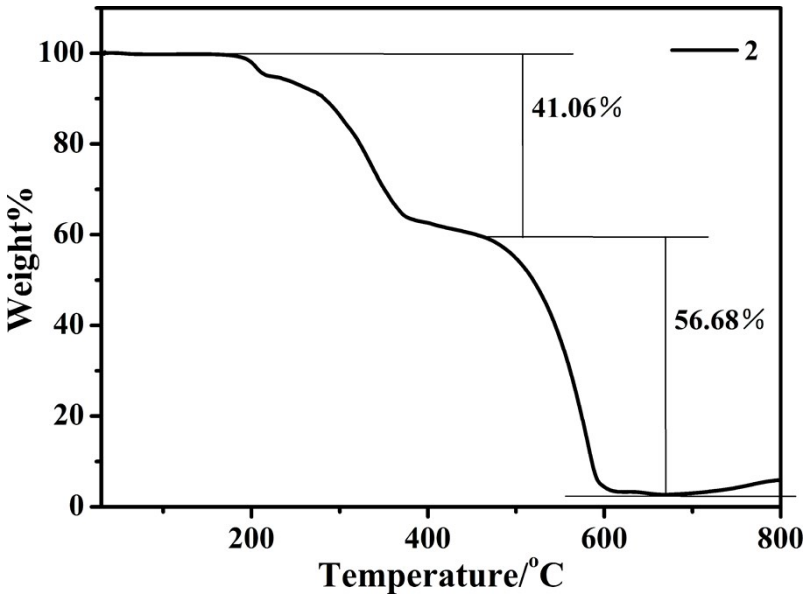

(b)

Fig. S1 Thermogravimetric (TG) curves of **1** and **2**.

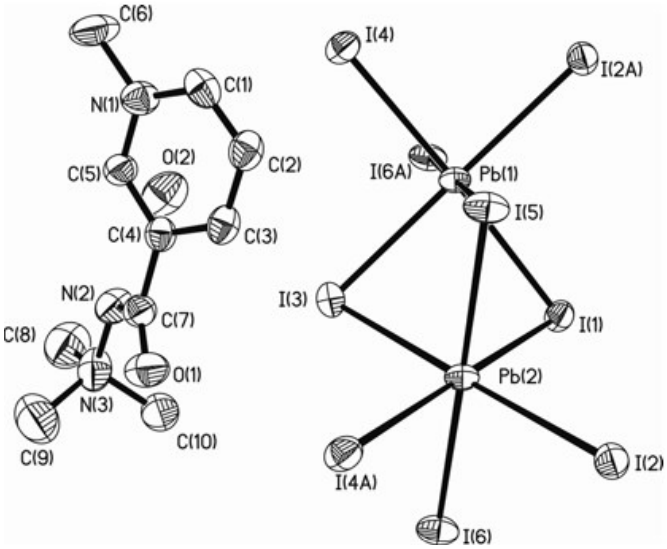

Compound **1**

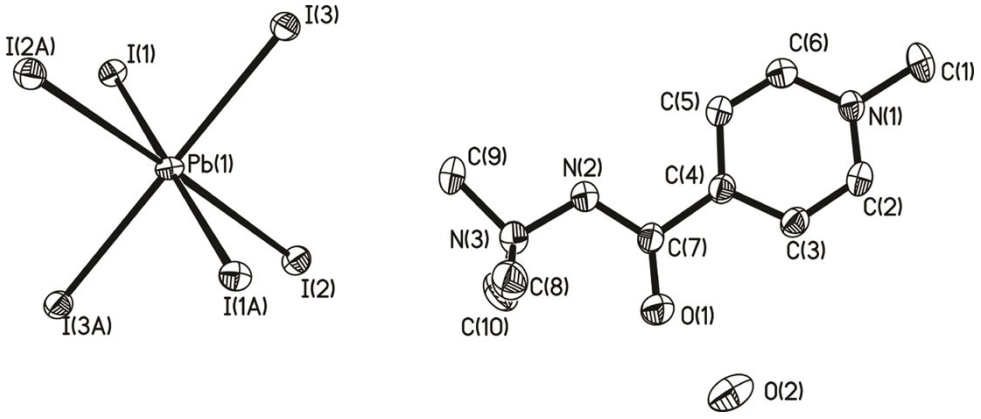

Compound **2**

Fig. S2 The asymmetric units of **1** and **2**.

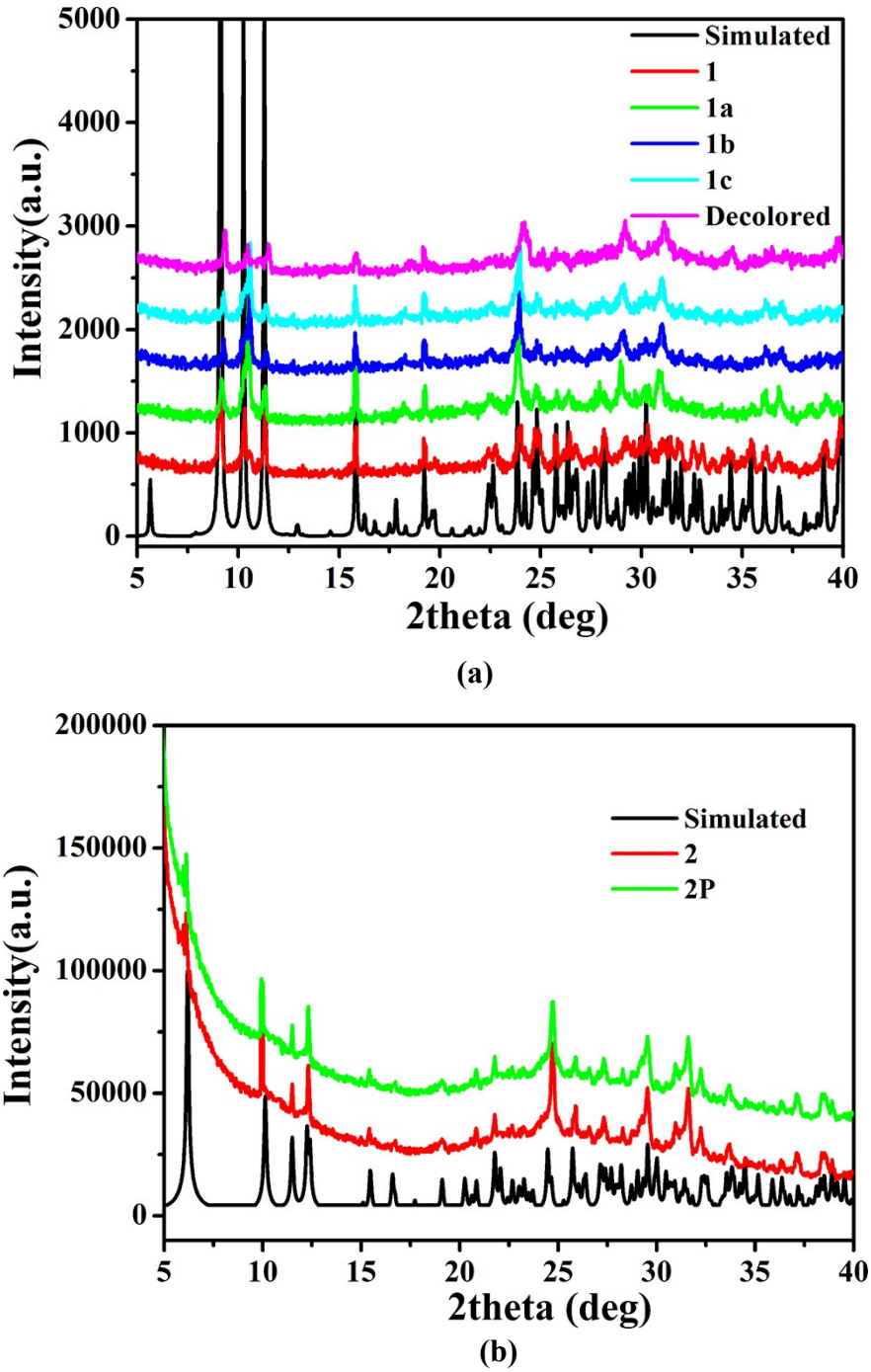

Fig. S3 Powder X-ray diffraction (PXRD) patterns of **1** and **2**.

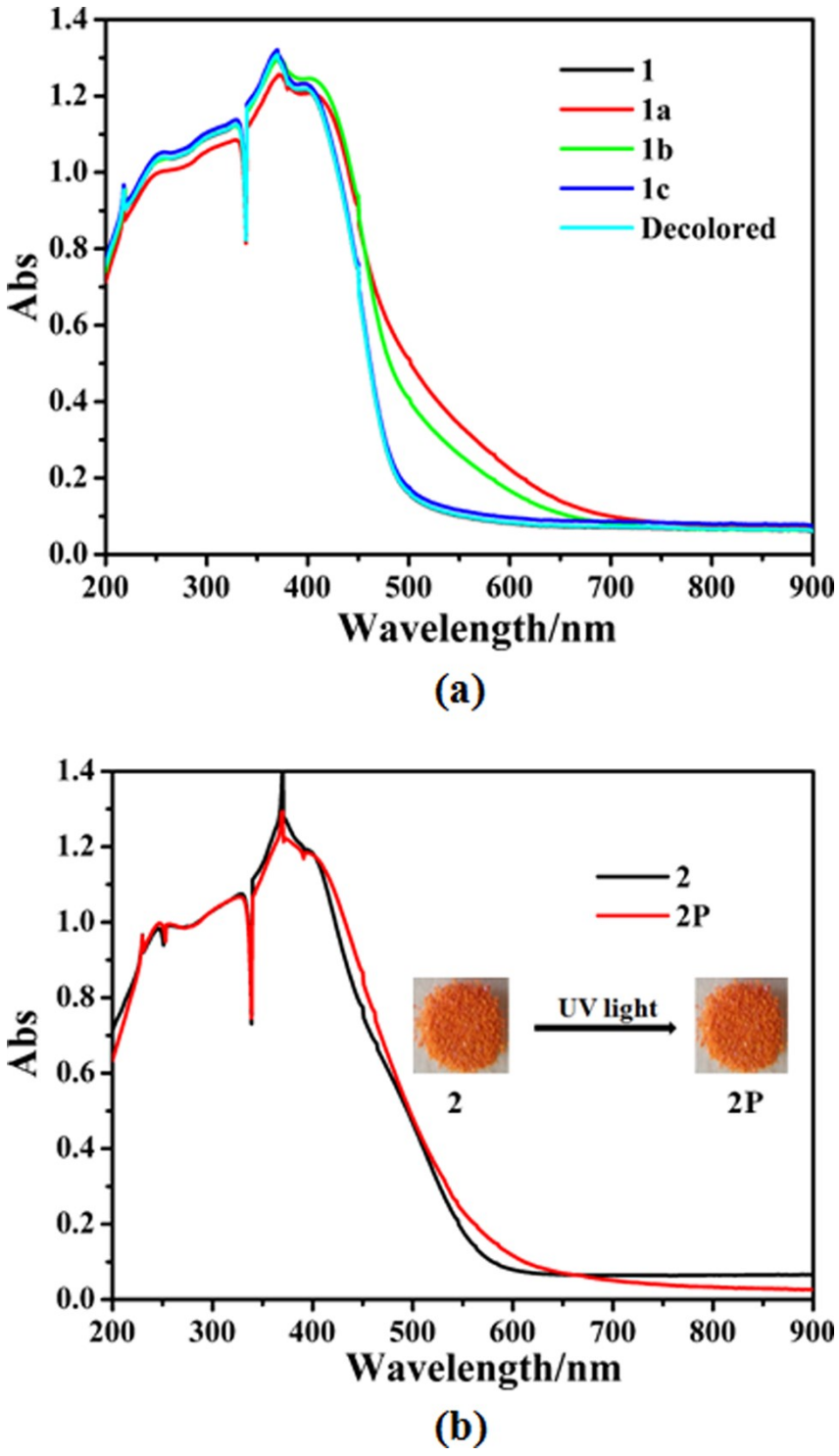

Fig. S4 UV-vis absorption spectra of **1** and **2** before and after irradiation.

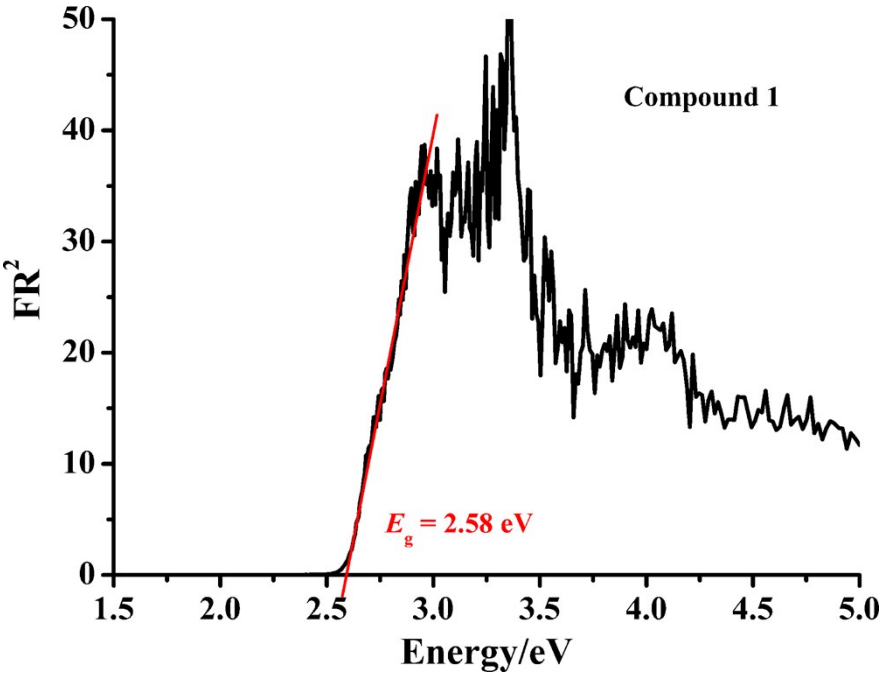

(a)

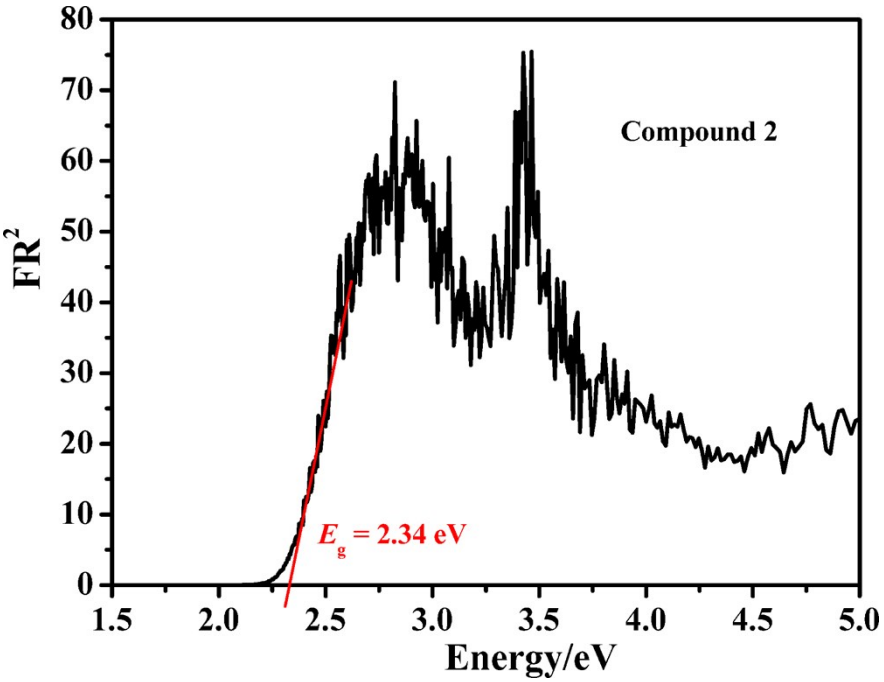

(b)

Fig. S5 Optical band gaps of **1** and **2**

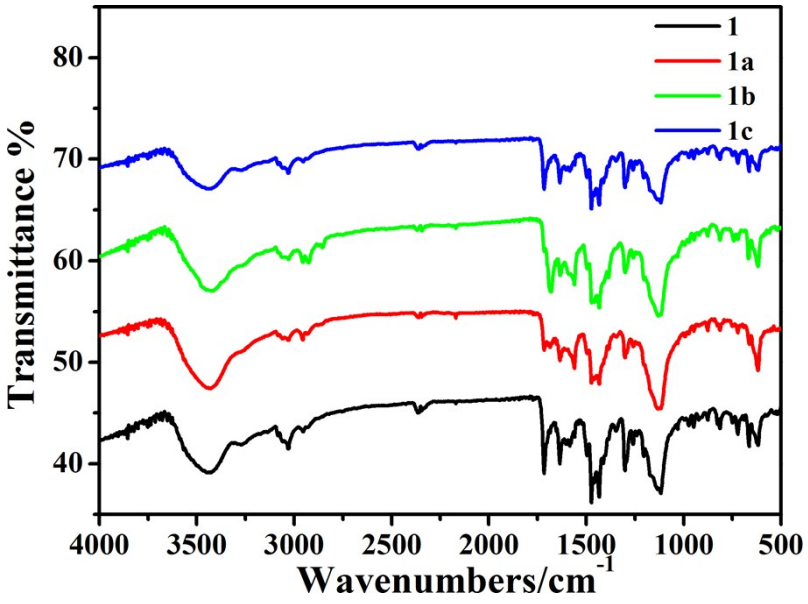

(a)

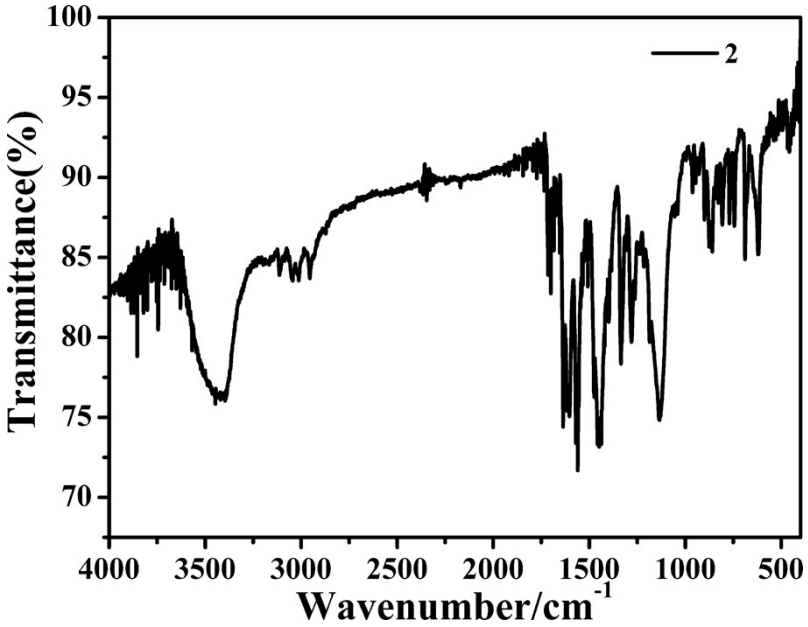

(b)

Fig. S6 IR spectra of **1** and **2** before and after irradiation

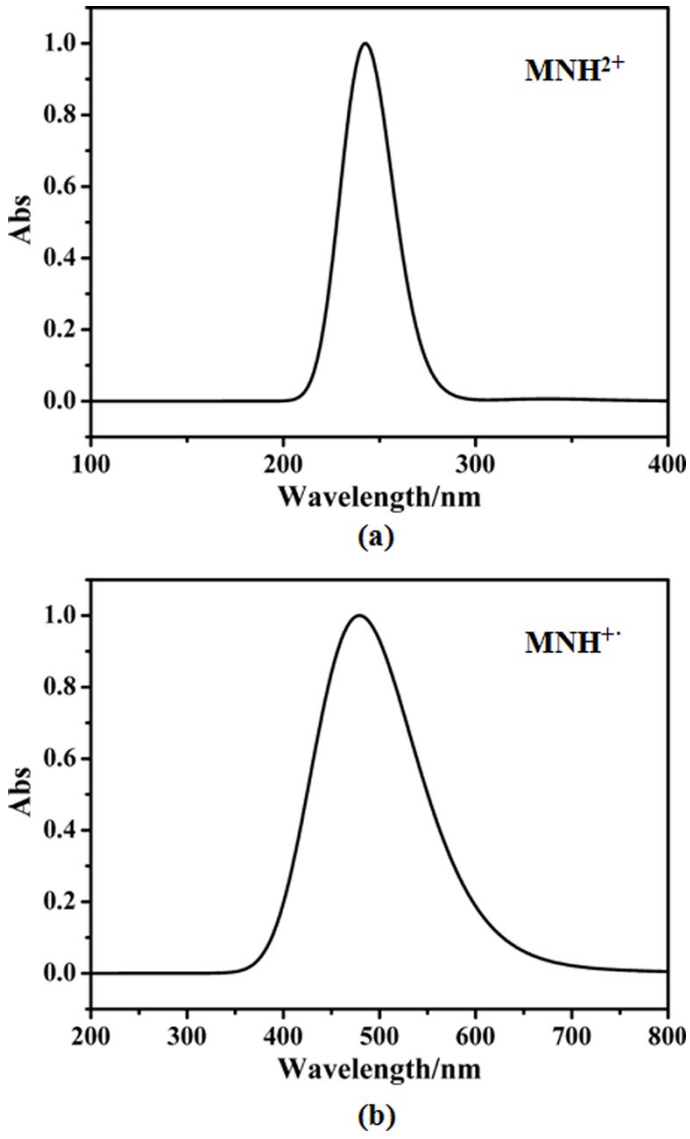

Fig. S7 The calculated UV-vis spectra of $[MNH]^{2+}$ cation (a) and $[MNH]^{+\bullet}$ radical (b) through density functional theory (DFT) computations using the Gaussian 09 suite of programs[1]. A hybrid functional B3LYP was used for all calculations.

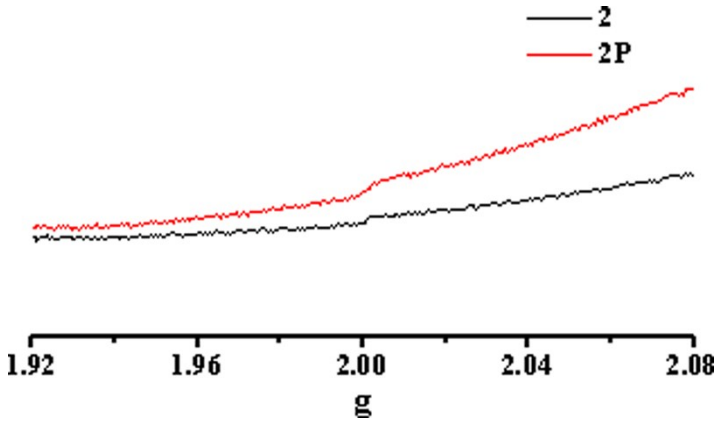

Fig. S8 EPR spectra of **2** before and after irradiation

2. Tables

Table S1 Crystallographic data and refinement parameters of **1** and **2**

Compound	**1**	**2**
CCDC code	1975873	2016978
Temperature (K)	273(2)	273(2)
Empirical formula	$C_{20}H_{34}N_6O_3Pb_4I_{12}$	$C_{10}H_{17}N_3O_2PbI_3$
Formula weight	2758.13	799.16
Crystal size (mm)	0.52 x 0.12 x 0.01	0.56 x 0.082 x 0.018
Crystal system	Triclinic	Monoclinic
Space group	$P\bar{1}$	$P2(1)/c$
a (Å)	7.9265(6)	14.2985(9)
b (Å)	11.5631(9)	7.9199(5)
c (Å)	15.8748(12)	17.4889(12)
α (°)	81.696(2)	90
β (°)	83.649(2)	94.076(2)
γ (°)	77.133(2)	90
V (Å^3)	1398.95(19)	1975.5(2)
Z	1	4
D_c (g cm^{-3})	3.274	2.690
F(000)	1184	1424
μ (mm^{-1})	18.644	13.230
θ range (°)	2.85 to 28.39	2.33 to 28.37
Reflections collected	25156	26964
Unique reflections	7030	4928
R_{int}	0.0410	0.0296
Goodness-of-fit on F^2	1.022	1.240
R_1/wR_2, $[I \geq 2\sigma(I)]$[a,b]	0.0413/0.1050	0.0264/0.0759
R_1/wR_2, (all data)	0.0703/0.1180	0.0412/0.0960
$\Delta\rho_{max}/\Delta\rho_{min}$ (e Å^{-3})	1.903/-1.395	1.525/-2.021

[a] $R_1 = \sum||F_o|-|F_c||/\sum|F_o|$ [b] $wR_2 = [\sum w(F_o^2-F_c^2)^2/\sum w(F_o^2)^2]^{1/2}$

Table S2 Selected distances (Å) and angles (°) of **1** and **2**

Compound **1**			
Pb(1)-I(5)	3.1667(7)	Pb(1)-I(3)	3.1881(8)
Pb(1)-I(4)	3.1931(7)	Pb(1)-I(2)#1	3.2420(8)
Pb(1)-I(1)	3.2648(7)	Pb(1)-I(6)#1	3.2749(8)
Pb(2)-I(2)	3.2129(8)	Pb(2)-I(5)	3.2160(7)
Pb(2)-I(3)	3.2172(8)	Pb(2)-I(1)	3.2223(8)
Pb(2)-I(4)#2	3.2294(8)	Pb(2)-I(6)	3.2424(8)
I(2)-Pb(1)#2	3.2420(8)		
I(4)-Pb(2)#1	3.2294(8)	I(6)-Pb(1)#2	3.2749(8)
I(5)-Pb(1)-I(3)	86.77(2)	I(5)-Pb(1)-I(4)	94.74(2)
I(3)-Pb(1)-I(4)	93.53(2)	I(5)-Pb(1)-I(2)#1	93.17(2)
I(3)-Pb(1)-I(2)#1	179.58(2)	I(4)-Pb(1)-I(2)#1	86.88(2)
I(5)-Pb(1)-I(1)	86.77(2)	I(3)-Pb(1)-I(1)	83.918(19)
I(4)-Pb(1)-I(1)	176.97(2)	I(2)#1-Pb(1)-I(1)	95.67(2)
I(5)-Pb(1)-I(6)#1	179.65(2)	I(3)-Pb(1)-I(6)#1	93.02(2)
I(4)-Pb(1)-I(6)#1	85.55(2)	I(2)#1-Pb(1)-I(6)#1	87.04(2)
I(1)-Pb(1)-I(6)#1	92.93(2)	I(2)-Pb(2)-I(5)	93.78(2)
I(2)-Pb(2)-I(3)	178.79(2)	I(5)-Pb(2)-I(3)	85.46(2)
I(2)-Pb(2)-I(1)	94.88(2)	I(5)-Pb(2)-I(1)	86.67(2)
I(3)-Pb(2)-I(1)	84.142(19)	I(2)-Pb(2)-I(4)#2	86.76(2)
I(5)-Pb(2)-I(4)#2	96.03(2)	I(3)-Pb(2)-I(4)#2	94.25(2)
I(1)-Pb(2)-I(4)#2	176.75(2)	I(2)-Pb(2)-I(6)	88.08(2)
I(5)-Pb(2)-I(6)	177.658(19)	I(3)-Pb(2)-I(6)	92.67(2)
I(1)-Pb(2)-I(6)	91.75(2)	I(4)#2-Pb(2)-I(6)	85.50(2)
Pb(2)-I(1)-Pb(1)	75.718(17)	Pb(2)-I(2)-Pb(1)#2	75.347(17)
Pb(1)-I(3)-Pb(2)	76.862(17)	Pb(1)-I(4)-Pb(2)#1	75.794(18)
Pb(1)-I(5)-Pb(2)	77.182(17)	Pb(2)-I(6)-Pb(1)#2	74.503(17)

Compound **2**			
Pb(1)-I(1)	3.2265(5)	Pb(1)-I(2)	3.2825(5)
Pb(1)-I(1)#2	3.2379(5)	Pb(1)-I(2)#1	3.1875(5)
Pb(1)-I(3)	3.2322(5)	Pb(1)-I(3)#2	3.2077(5)
I(1)-Pb(1)#1	3.2379(5)	I(2)-Pb(1)#2	3.1875(5)
I(3)-Pb(1)#1	3.2077(5)		
I(1)-Pb(1)-I(2)	97.378(13)	I(1)-Pb(1)-I(3)	89.290(12)
I(1)-Pb(1)-I(1)#2	179.535(12)	I(1)#2-Pb(1)-I(2)	82.776(12)
I(2)#1-Pb(1)-I(3)#2	93.539(13)	I(2)#1-Pb(1)-I(1)	84.462(12)
I(2)#1-Pb(1)-I(3)	86.375(13)	I(2)#1-Pb(1)-I(1)#2	95.393(13)
I(2)#1-Pb(1)-I(2)	177.782(13)	I(3)#2-Pb(1)-I(1)	90.929(13)
I(3)#2-Pb(1)-I(3)	179.756(9)	I(3)-Pb(1)-I(1)#2	90.260(12)
I(3)#2-Pb(1)-I(2)	85.207(12)	I(3)-Pb(1)-I(2)	94.871(13)
I(3)#2-Pb(1)-I(1)#2	89.521(12)	Pb(1)-I(1)-Pb(1)#1	75.554(10)
Pb(1)#2-I(2)-Pb(1)	75.462(10)	Pb(1)#1-I(3)-Pb(1)	75.891(11)

Symmetry code: for **1**: #1 x-1,y,z; #2 x+1,y,z; for **2**: #1 -x+2,y-1/2,-z+1/2; #2 -x+2,y+1/2,-z+1/2.

Table S3. Density functional theory (DFT) calculations for two cations

Organic cations	LUMO (eV)	HOMO (eV)
Methylated nicotinohydrazide (MNH^{2+})	-9.7126	-15.1177
Methylated isonicotinohydrazide ($MINH^{2+}$)	-10.1181	-15.0970

[a]The density functional theory (DFT) calculations were carried out with the Gaussian 09 suite of programs[1]. A hybrid functional B3LYP was used for all calculations. Geometry was optimized using the 6-31G basis set.

Reference

[1] M. J. Frisch, G. W. Trucks, H. B. Schlegel, G. E. Scuseria, M. A. Robb, J. R. Cheeseman, G. Scalmani, V. Barone, B. Mennucci, G. A. Petersson, H. Nakatsuji, M. Caricato, X. Li, H. P. Hratchian, A. F. Izmaylov, J. Bloino, G. Zheng, J. L. Sonnenberg, M. Hada, M. Ehara, K. Toyota, R. Fukuda, J. Hasegawa, M. Ishida, T. Nakajima, Y. Honda, O. Kitao, H. Nakai, T. Vreven, J. A. Montgomery, Jr., J. E. Peralta, F. Ogliaro, M. Bearpark, J. J. Heyd, E. Brothers, K. N. Kudin, V. N. Staroverov, T. Keith, R. Kobayashi, J. Normand, K. Raghavachari, A. Rendell, J. C. Burant, S. S. Iyengar, J. Tomasi, M. Cossi, N. Rega, J. M. Millam, M. Klene, J. E. Knox, J. B. Cross, V. Bakken, C. Adamo, J. Jaramillo, R. Gomperts, R. E. Stratmann, O. Yazyev, A. J. Austin, R. Cammi, C. Pomelli, J. W. Ochterski, R. L. Martin, K. Morokuma, V. G. Zakrzewski, G. A. Voth, P. Salvador, J. J. Dannenberg, S. Dapprich, A. D. Daniels, O. Farkas, J. B. Foresman, J. V. Ortiz, J. Cioslowski, and D. J. Fox, Gaussian 09, Revision D.01, Gaussian Inc., Wallingford, CT, 2013.